

Dust-induced changes in phytoplankton composition in the Tasman Sea during the last four glacial cycles

Eva Calvo¹ and Carles Pelejero¹

Research School of Earth Sciences, Australian National University, Canberra, ACT, Australia

Graham A. Logan

Petroleum and Marine Division, Geosciences Australia, Canberra, ACT, Australia

Patrick De Deckker

Department of Geology, Australian National University, Canberra, ACT, Australia

Received 26 November 2003; revised 16 February 2004; accepted 23 March 2004; published 15 June 2004.

[1] An increase in iron supply associated with enhanced dust inputs could be responsible for higher marine phytoplankton production leading to the typically lower glacial atmospheric CO₂ concentrations, as suggested by the “iron hypothesis.” The enhanced dust supply may also have provided the oceans with significant amounts of silica, which would have favored the growth of diatoms over coccolithophores, as suggested by the “silica hypothesis.” Here we present new data on molecular biomarkers in a sediment core from the midlatitudes of the Southern Hemisphere, which reveal dust-induced changes in the relative contribution of the phytoplankton to total productivity. Our results illustrate a shift in the relative abundance of siliceous over calcareous organisms during glacial times, when terrestrial aeolian input was enhanced. Although we did not detect a significant glacial decrease in coccolithophorid productivity, the decrease in the CaCO₃/Corg rain ratio could have still contributed to some extent in lowering atmospheric CO₂ levels. *INDEX TERMS:* 1055 Geochemistry: Organic geochemistry; 1615 Global Change: Biogeochemical processes (4805); 4267 Oceanography: General: Paleooceanography; *KEYWORDS:* dust, ocean carbon cycle, marine productivity

Citation: Calvo, E., C. Pelejero, G. A. Logan, and P. De Deckker (2004), Dust-induced changes in phytoplankton composition in the Tasman Sea during the last four glacial cycles, *Paleoceanography*, 19, PA2020, doi:10.1029/2003PA000992.

1. Introduction

[2] The Southern Ocean has long been recognized as playing a key role in driving the major CO₂ changes observed during glacial/interglacial cycles [Knox and McElroy, 1984; Martin and Fitzwater, 1988; Petit *et al.*, 1999; Sarmiento and Toggweiler, 1984]. Today, this ocean is characterized by high nutrients levels which are not fully utilized by phytoplankton. The low productivity appears to be due to low iron levels, which significantly inhibits phytoplankton growth [Martin *et al.*, 1990]. In situ iron-enrichment experiments have confirmed that the addition of iron to areas like the Southern Ocean (the so-called high-nutrient, low-chlorophyll (HNLC) areas), where aeolian iron input is among the lowest in the world oceans [Mahowald *et al.*, 1999], greatly enhances phytoplankton productivity [Boyd *et al.*, 2000; Coale *et al.*, 1996; Martin *et al.*, 1994; Tsuda *et al.*, 2003]. During glacial times, the more arid and dustier conditions supplied the Southern Ocean (today's largest HNLC region) with 10 to 50 times more iron [Kumar *et al.*, 1995; Mahowald *et al.*, 1999; Martin

and Fitzwater, 1988; Petit *et al.*, 1999]. This would have stimulated the biological pump with the subsequent draw-down of dissolved CO₂ [Martin, 1990]. However, an enhanced biological production during glacial times is not fully supported by palaeoceanographic data. Alternative hypotheses such as increased water stratification or enhanced sea-ice coverage have been proposed to explain low glacial atmospheric CO₂ (see review by Anderson *et al.* [2002]). Moreover, there is still no evidence of the ultimate fate of the CO₂ that was taken up by the enhanced algal blooms that occurred after the fertilization experiments. No significant increase of iron-derived export production and, therefore, efficient CO₂ drawdown was detected during these experiments [Boyd *et al.*, 2000].

[3] Complementary to the “iron hypothesis,” Harrison [2000] proposed the “silica hypothesis” which does not require further changes in total productivity, but a change in phytoplankton community, namely diatoms and coccolithophores. Both siliceous and nonsiliceous organisms remove dissolved CO₂ during photosynthesis. However, the secretion of coccolith calcite skeletons (CaCO₃) results in an increase in *p*CO₂, whereas the siliceous diatom frustules represent a net drawdown of this greenhouse gas, solely incorporated as organic matter. The contribution of diatoms to total biological production largely depends on the availability of silicic acid: when Si(OH)₄ is not limited, diatom

¹Also at Petroleum and Marine Division, Geosciences Australia, Canberra, ACT, Australia.

production is favored over coccolithophores [Egge and Aksnes, 1992]. Increased silicate dust availability during glacial times [Harrison, 2000] or, alternatively, a more efficient distribution of Si-rich glacial Antarctic waters [Brzezinski et al., 2002; Matsumoto et al., 2002] or increased riverine input [Tréguer et al., 1995; Tréguer and Pondaven, 2000] may have resulted in a major increase in diatom productivity and a decrease in coccolithophores. This could potentially explain the observed glacial/interglacial CO₂ cycles through a decrease in calcite production and, in turn, in the CaCO₃/organic carbon rain ratio reaching the seafloor. A decrease in the “rain ratio,” due to a decrease in the export of calcium carbonate or an increase in organic matter production, would lead to a change in ocean alkalinity and pH and thus in pCO₂ [Archer and Maier-Reimer, 1994]. This scenario would be particularly effective in modern low-Si waters, such as the subantarctic and subtropical regions where coccolithophores dominate primary productivity [Brzezinski et al., 2002]. Furthermore, in situ Fe fertilization [Watson et al., 2000] and bottle experiments [Franck et al., 2000; Hutchins and Bruland, 1998; Takeda, 1998] have also shown that the addition of iron not only enhances diatom growth over other taxa, but also decreases the Si:N uptake ratios. This phenomenon makes diatoms more efficient at removing surface dissolved CO₂, thus exporting more organic carbon per unit of buried opal. There is still no evidence in the palaeorecord, however, of such a shift in the phytoplanktonic community between glacial and interglacial times.

[4] In order to test whether changes in phytoplankton taxa took place during glacial times, we studied a marine sediment core retrieved from off southeast Australia. It covers the last four glacial/interglacial cycles and has been investigated by means of terrestrial and marine molecular biomarkers. Our results show glacial/interglacial shifts in the relative contribution of diatoms and coccolithophores to total phytoplankton productivity. These shifts are strongly correlated with changes in dust input. A previous study based on molecular biomarkers in a southern Caribbean core illustrated the potential of this palaeoceanographic tool to reconstruct past changes in phytoplankton composition, showing a shift from diatoms to coccolithophores during the transition from the Younger Dryas cold period to the Holocene [Werne et al., 2000].

2. Oceanographic Setting

[5] Core Fr94-GC3 was recovered from the east Tasman Plateau and it has already been the focus of other palaeoceanographic studies [Hiramatsu and De Deckker, 1997; Nees, 1997]. It is located north of the present position of the subtropical front (STF; 44°15'S, 149°59'E, 2667 m water depth; Figure 1), which separates warm and saltier subtropical waters from the cold, less saline and nutrient rich subantarctic waters of the Southern Ocean [Rintoul et al., 1997; Wyrki, 1962]. In the Tasman Sea, the STF is not a well-marked frontal structure, but a broadly branched front of temperature and salinity gradients centered around 45°–47°S, which varies in time (see Belkin and Gordon [1996] for a summary of different criteria for STF identification).

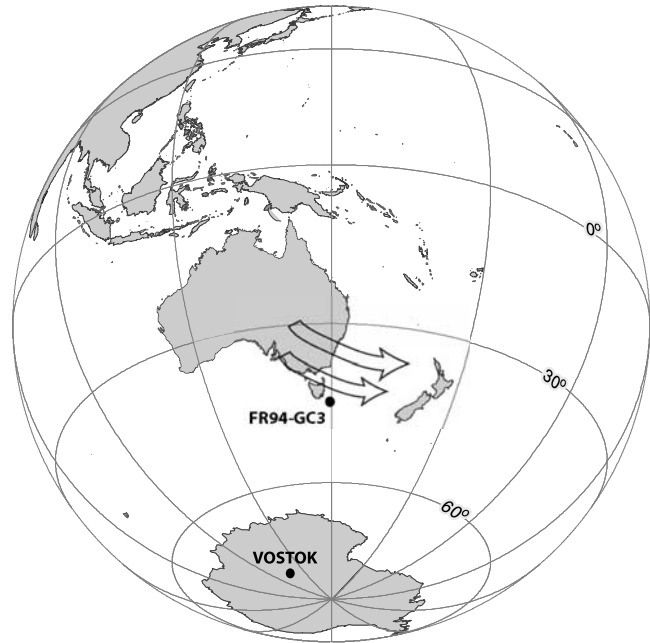


Figure 1. Locations of core Fr94-GC3 in the east Tasman Plateau and Antarctic Vostok ice core. Arrows indicate the source and path of dust reaching the Tasman Sea [Hesse, 1994].

During glacial times, the STF only moved slightly equatorward in the vicinity of the east Tasman Plateau [Martinez, 1994; Nees, 1997; Passlow et al., 1997]. On the basis of the abundance of left-coiling *Neogloboquadrina pachyderma*, the STF location was inferred north of 43°S during glacial marine isotope stages (MIS) 6, 10 and 12 [Martinez, 1994] and around 45°S during the last glacial period [Passlow et al., 1997]. In this area, changes in productivity over glacial/interglacial times have been associated either with (1) the presence and migration of the STF over the location of the studied cores [Nees et al., 1999; Passlow et al., 1997], (2) an intensification of eddy formation associated with the southward flow of the east Australian Current [Nees, 1997] or (3) an increase in dust supply to surface waters [Ikehara et al., 2000; Nees et al., 1999]. As described in section 4, our data give support to this last mechanism as being the most important in fertilizing surface waters of the south Tasman Sea. Since the STF is located near our core location, productivity changes associated with migration of the front cannot be completely ruled out. However, it is important to note that both subtropical and subantarctic waters south of Australia have low concentrations of dissolved Fe and Si which could limit primary production [Sedwick et al., 1997]. Hence changes in productivity due to migrations of the STF are not expected to be as important as, for instance, those associated with the movement of the strong north-south Si gradient related with the polar front (55–57°S), further south of our core location.

3. Methods

[6] The age model was established by comparing the oxygen isotope record of the planktonic foraminifera *Glo-*

bigerina bulloides to the global SPECMAP isotope curve [Imbrie et al., 1984; Martinson et al., 1987], which provides an average sedimentation rate of 1.2 cm/kyr for the last 450 kyr. There are no drastic changes in sedimentation rate, but minor artificial fluctuations may exist due to possible inaccuracies of the age model, which are inherent to any record older than 40 kyr, beyond the limit of radiocarbon dating. For this reason, and to avoid ambiguous calculations based on age model-dependent mass accumulation rates [e.g., Pelejero, 2003], absolute biomarker concentrations have been used instead.

[7] Analysis and characterization of total lipid content, together with U_{37}^K sea surface temperature (SST) estimations were performed at Geoscience Australia laboratories following published methods [Calvo et al., 2003]. Briefly, 3–4 g of freeze-dried sediment were loaded into 11 mL stainless steel extraction cells of a Dionex ASE 200 pressurized liquid extraction system. After addition of an internal standard (*n*-hexatriacontane) and subsequent extraction with dichloromethane, the extracts (~25 ml) were evaporated to dryness under a nitrogen stream. Six percent potassium hydroxide in methanol was used to hydrolyze wax esters and eliminate interferences during quantitation of gas chromatographic data. After derivatization with bis(trimethylsilyl) trifluoroacetamide, extracts were dissolved in toluene and then injected in a Hewlett Packard HP6890 Gas Chromatograph with a flame ionization detector and equipped with a CP-Sil 5 CB capillary column (50 m, 0.32 mm I.D. and 0.12 mm film thickness). The oven was programmed from 90°C (holding time of 1 min) to 160°C at 15°C/min, 160°C to 280°C at 10°C/min with 30 min hold at 280°C and finally, from 280°C to 310°C at 6°C/min with a holding time of 6 min. Triplicate extraction and analyses of a marine sediment with similar alkenone content gave an analytical estimated uncertainty of $\pm 0.04^\circ\text{C}$. Selected samples were analyzed by GC-MS for compound identification, using a Hewlett-Packard HP5973 MSD attached to an HP6890 GC and with the same capillary column. The mass spectrometer was operated at 70 eV in full scan mode from 50 to 600 m/z.

4. Results and Discussion

[8] Several key marine and terrestrial organic tracers were analyzed to assess changes in the source of organic matter and, in particular, in the relative contribution of the different phytoplanktonic taxa to primary productivity. We used long-chain odd *n*-alkanes (C_{25} – C_{31}) derived from terrestrial higher plants [Eglinton and Hamilton, 1967] as tracers of terrestrial input to the marine environment. Long chain alkenones were used to trace Haptophyta algae input, such as the coccolithophore *Emiliania huxleyi*, the most abundant source of alkenones in today's ocean waters [Brassell, 1993]. Changes in alkenone concentrations provided qualitative information of past productivity of coccolithophorid algae [Pailler et al., 2002; Villanueva et al., 2001]. In the same manner, 24-methylcholesta-5,22-dien-3 β -ol has been used as a proxy for diatom abundances [Schubert et al., 1998; Schulte et al., 1999; Werne et al., 2000]. However, this compound can also be synthesized by some Haptophyta algae and thus, although it represents the major sterol in

most species of diatoms, it may not be a specific tracer for diatom productivity [Volkman, 1986]. In this work, we focus on periods when decoupling occurs between the alkenone and 24-methylcholesta-5,22-dien-3 β -ol records, as this phenomenon implies that the sources of these biomarkers must have been different (see further discussion below). Hereafter, the term “brassicasterol” will be used instead of 24-methylcholesta-5,22-dien-3 β -ol, for simplification. However, it should be noted that, strictly speaking, the term “brassicasterol” refers exclusively to the compound with the β stereochemistry at C_{24} , while epibrassicasterol is the name given to the α -isomer. The two isomers cannot be separated by the gas chromatographic columns commonly used in palaeoceanographic studies. Additionally, two more sterols have been analyzed: dinosterol (4 α , 23, 24-trimethyl-5 α -cholest-22-en-3 β -ol), a marker for dinoflagellate input [Boon et al., 1979] and cholesterol (cholest-5-en-3 β -ol) which is normally ascribed to zooplankton, although it can also be synthesized by a wide variety of phytoplankton [Volkman, 1986].

4.1. Terrestrial *n*-Alkanes

[9] In core Fr94-GC3, a strong predominance of odd versus even carbon-numbered *n*-alkanes is encountered, with an average carbon preference index of 5.9, indicating origin from higher plants [Peltzer and Gagosian, 1989]. An aeolian transport of the *n*-alkanes is supported by the absence of major rivers and the location of the core under the influence of westerly winds, which brings dust to the Tasman Sea from southeastern Australia and Tasmania [Hesse, 1994]. Indeed, atmospheric transport of *n*-alkanes originating in Australia has also been recognized in aerosol samples from New Zealand, 1500 km from east Australia [Gagosian et al., 1987].

[10] Over the last 450 kyr, terrestrial *n*-alkane (C_{25} , C_{27} , C_{29} and C_{31}) concentrations display a clear glacial-interglacial pattern, with the highest values recorded during glacial times (Figure 2b, note reverse axis). This record of terrestrial input is inversely correlated with the long- and short-term trends exhibited by SST based on the U_{37}^K (C. Pelejero et al., manuscript in preparation, 2004) suggesting a strong link between climate and dust input. Measurements of aeolian grain size in the same core corroborate this link, displaying larger quartz grains during glacial times and thus substantiating the prevalence of stronger winds (M. MacPhail and P. De Deckker, unpublished data, 2000). The Vostok dust record for the last 420 kyr shows a remarkable increase in dust content during glacial periods (Figure 3c), which has been associated with a global increase in continental aridity and more vigorous atmospheric circulation bringing also larger dust particles to Antarctica [Petit et al., 1999]. The good parallelism between our *n*-alkane record and the dust content in Vostok indicates that the climatic changes observed south of Tasmania were not only restricted to that region.

[11] The C_{31} *n*-alkane homologue is the most predominant of all the *n*-alkanes, representing 41% and 58% of the total *n*-alkanes during interglacial and glacial periods, respectively. The increased abundance of the *n*- C_{31} during glacial times, with respect to shorter chain compounds (C_{29}

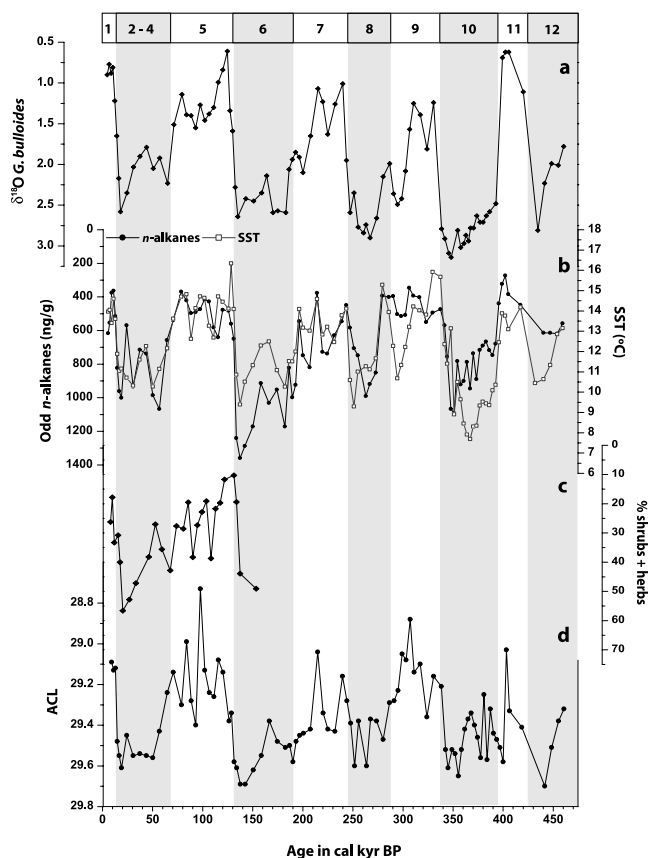


Figure 2. (a) The $\delta^{18}\text{O}$ record of planktonic foraminifera *Globigerina bulloides* used to establish the age model. (b) Comparison of U_{37}^K - SST estimations with C_{25} to C_{31} odd *n*-alkane concentrations used as proxy of terrestrial input (note reverse axis). Temperature minima are strongly correlated with higher inputs of continental material, very likely related to enhanced dust inputs. The global calibration from Müller *et al.* [1998] has been used to translate U_{37}^K values into SST. (c) Percent pollen derived from shrubs and herbs (M. MacPhail and P. De Deckker, unpublished data, 2000). (d) Average chain length (ACL) ($\text{ACL} = ([C_{25}] \times 25 + [C_{27}] \times 27 + [C_{29}] \times 29 + [C_{31}] \times 31) / ([C_{25}] + [C_{27}] + [C_{29}] + [C_{31}])$) as an indicator of continental aridity. Gray shaded areas denote glacial periods.

and C_{27}), is reflected in the average chain length (ACL) index (Figure 2d). This index is used as a proxy for changes in the vegetation type within the source area or a change in the source region itself [Cranwell, 1973; Cranwell *et al.*, 1987; Gagosian *et al.*, 1987]. In previous studies, longer chain length alkanes (high ACL) have been associated with vegetation from warm tropical areas, whereas a low ACL is associated with plants input from cooler regions [Peltzer and Gagosian, 1989; Poynter *et al.*, 1989]. However, the ACL relationship with temperature does not seem to operate in core Fr94-GC3. We observe consistent higher ACL values during cold, glacial times and lower values during interglacial periods (Figure 2d). An alternative explanation to the observed ACL changes would be a physiological

plant response to more arid conditions during glacial periods. The *n*-alkanes are major components of epicuticular waxes of higher plants and their main function is to prevent them from water loss. Studies on hydrocarbon composition adaptation to environmental changes, such as drought stress, have shown a relationship between alkane chain length and plant permeability [Dodd *et al.*, 1998; Dodd and Afzal-Rafii, 2000, and references therein]. Under water stress conditions (due to either high temperature or aridity), plants tend to synthesize longer chain length alkanes in order to provide a more efficient wax coating.

[12] On the other hand, alkane distribution in lake sediments have also shown to be indicative of the type of vegetation in the drainage basin, with higher abundances of n - C_{31} associated with the development of grasses compared to trees [Cranwell, 1973; Cranwell *et al.*, 1987]. For example, Fischer *et al.* [2003] attributed the occurrence of longer chain *n*-alkanes in lake sediments to inputs from grasses associated with periods of deforestation, while shorter ACL compounds were encountered during periods of greater arboreal input from land. Pollen data from core Fr94-GC3, available only for the last 150 kyr, show an increase in the percentage of pollen derived from C4 plants (shrubs and herbs) versus C3 plants (rain forest and ferns) in glacial samples, reflecting a change in terrestrial plant cover toward more arid conditions (Figure 2c). Indications of drier conditions during the Last Glacial Maximum also come from a pollen record in a marine core offshore Victoria, southeastern Australia [Harle, 1997]. Alternatively, a change in the source area itself could also explain the variations observed in the ACL and pollen records. Although this possibility cannot be discarded, modeling studies suggest that the position of the westerlies over Australia has been similar during glacial times [Wyrwoll *et al.*, 2000]. If that is the case, and the source area has not changed, our data would more likely reflect changes in vegetation due to climate change.

[13] It is still not clear whether the wind system was stronger or continental aridity was enhanced during glacial times [Hesse and McTainsh, 1999] but, regardless the cause, *n*-alkane abundances in core Fr94-GC3 indicate that dust inputs, and thus associated iron and silica, are consistently higher during glacial periods.

4.2. Marine Biomarkers

[14] To assess links between dust input and the response of marine biota to the release of Fe and Si, *n*-alkane concentrations have been evaluated together with two marine productivity proxies, C_{37} alkenones and brassicasterol (Figures 3a and 3b). The response of the phytoplankton community to dust inputs seems to have been different during glacial MIS 10 compared to the last 330 kyr BP. For the oldest part of the record, all three biomarkers exhibit the same temporal evolution with a marked maximum during glacial MIS 10, giving support to an enhanced marine productivity as a result of increased terrestrial aeolian input. However, due to the parallel trends in the alkenone and brassicasterol records, assessment of differences between diatom and coccolithophorid productivity is not possible during this glacial stage. Since Haptophyta algae can

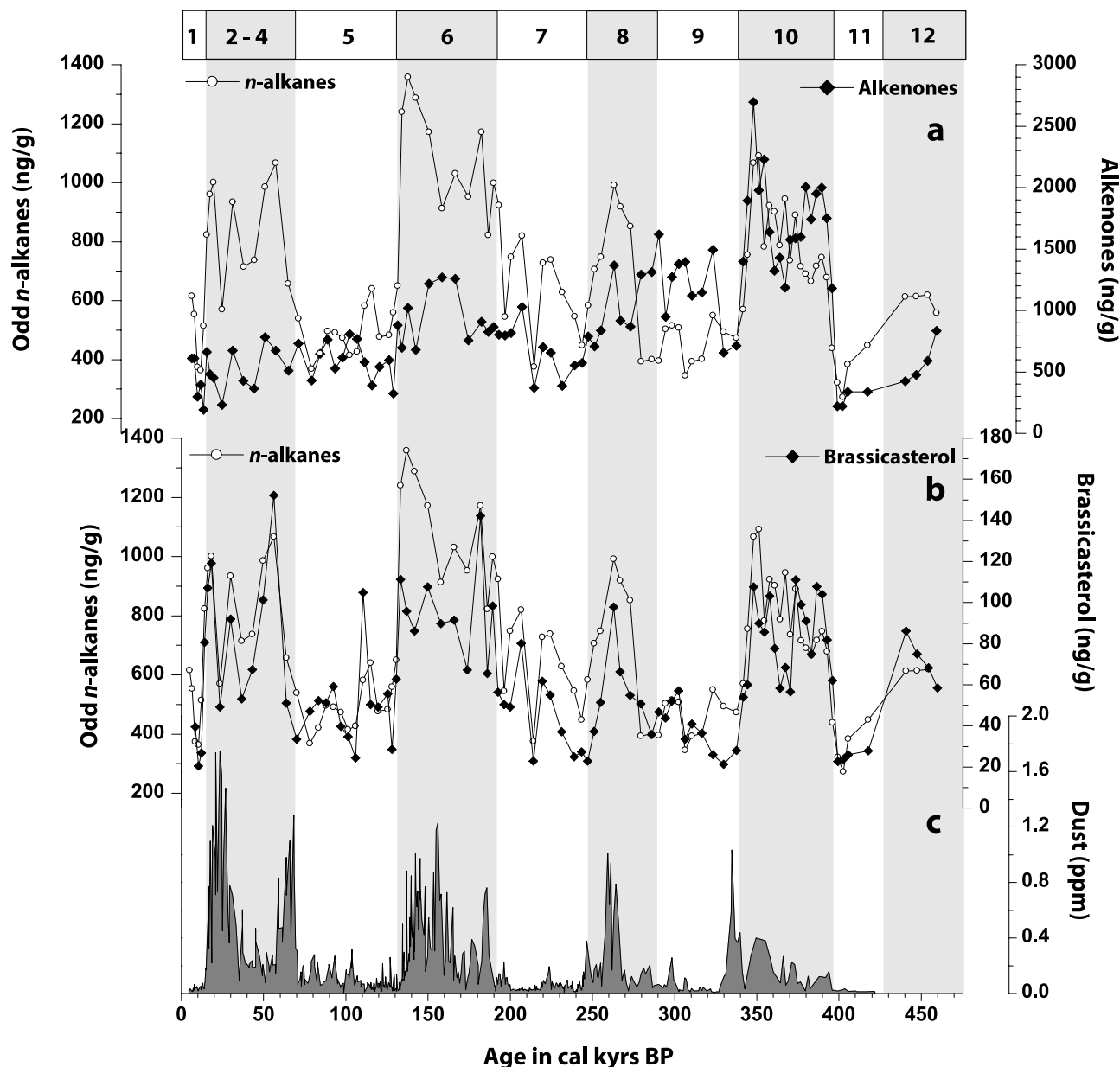


Figure 3. Total odd *n*-alkane abundances compared with two marine biomarkers. (a) C_{37} alkenones and (b) brassicasterol. While brassicasterol and total odd *n*-alkanes follow a clear glacial/interglacial pattern, C_{37} alkenone concentrations show no response to the main orbital parameters (see Figure 4). (c) Dust concentration as recorded in the Vostok ice core [Petit *et al.*, 1999]. The mismatching with our *n*-alkane record during glacial MIS 10 is likely due to difficulties in cross-correlating marine and ice cores.

contribute both brassicasterol and alkenones, the high abundances of C_{37} alkenones (>2000 ng/g) make it difficult to differentiate between the contribution of diatoms and coccolithophores to total productivity. In contrast, the period after 330 kyr BP is suitable to be studied by molecular biomarker comparison since a significant decoupling exists between brassicasterol and alkenones. Changes in the different contribution of haptophytes and diatoms to brassicasterol abundances can also be evaluated qualitatively looking at the brassicasterol/alkenone ratio. This ratio, which has been calculated after normalizing each

biomarker to its highest abundance value, should take higher values when diatoms predominate over haptophytes. Thus the gradual increase in brassicasterol/alkenone ratios observed for the youngest section of the record indicates the increasing importance of diatoms as the main source of brassicasterol.

[15] In core Fr94-GC3, brassicasterol abundances closely parallel the glacial/interglacial changes exhibited by *n*-alkanes, while C_{37} alkenone concentrations do not correlate with the terrestrial glacial/interglacial signal but follow a decreasing trend with the lowest values recorded

during the Holocene (Figure 3). Spectral analysis of these three biomarkers corroborates the different pattern that can be visually observed in these profiles (Figure 4). The *n*-alkanes and brassicasterol records show a strong response to orbital parameters of eccentricity (100 kyr cycle) and obliquity (41 kyr cycle), along with a third periodicity of about 30 kyr, which has been reported in aeolian records from the Pacific and Indian Oceans [Rea, 1994]. In contrast, C₃₇ alkenone content shows no coherence over any of the frequency bands observed by the *n*-alkanes and brassicasterol (Figure 4), indicating that these two phytoplankton communities responded differently to changes in dust input.

[16] In order to explore plausible mechanisms for the different pattern presented by the C₃₇ alkenone record, the effects of changes in the coccolithophorid species responsible for alkenone production are considered. The main alkenone producer in today's oceans is the coccolithophore *E. huxleyi*, but this alga first appeared about 270 kyr ago [Thierstein et al., 1977] and did not become abundant until late MIS 5. Prior to 270 ka, the most likely contributors of alkenones to marine sediments are the closely related species from the genus *Gephyrocapsa* [Marlowe et al., 1990]. Culture experiments have confirmed the existence of alkenones in the species *Gephyrocapsa oceanica* [Volkman et al., 1995; Sawada et al., 1996; Conte et al., 1998]. In Figure 5, available data on nannoplankton abundances for core Fr94-GC3 [Hiramatsu and De Deckker, 1997] are compared with alkenone concentrations in order to assess any possible influence of changes in alkenone-producing coccolithophores on the decreasing trend displayed by the biomarker record. A study in a marine core off Namibia found a positive correlation between alkenone concentrations and *Gephyrocapsa* spp. percentages, with the lowest alkenone concentrations occurring during the Holocene, when *Gephyrocapsa* spp. was also less abundant [Müller et al., 1997]. In core Fr94-GC3, *Gephyrocapsa* spp. are the most abundant coccolithophores through most of the record, with the exception of the last 30–40 kyr, when *E. huxleyi* became the predominant species (Figure 5). Thus it is very likely that *Gephyrocapsa* species were the responsible organism of the alkenone occurrence during most part of the record. However, the alkenone decreasing trend recorded in sediments of the Tasman Sea is not closely followed by a parallel decrease in the percentage of *Gephyrocapsa* spp, although there are some similarities during MIS 6 and 7. For instance, the high-alkenone abundances during MIS 10 do not correspond to higher percentages of *Gephyrocapsa* spp. A positive relationship between alkenone abundances and *Gephyrocapsa* spp. percentages would be expected if the amount of alkenones synthesized per coccolith was higher for *Gephyrocapsa* spp. than for *E. huxleyi*. Culture experiments, however, show similar production ratios of alkenone/algae cell, at least for *G. oceanica*, compared with *E. huxleyi* [e.g., Sawada et al., 1996]. Instead, the high-alkenone abundances observed during MIS 10 are more likely related to an increase in the total biomass of coccolithophores. Unfortunately, total coccolithophore abundances are not available from the original work done by Hiramatsu and De Deckker [1997], which was only focused on nannoplankton composition.

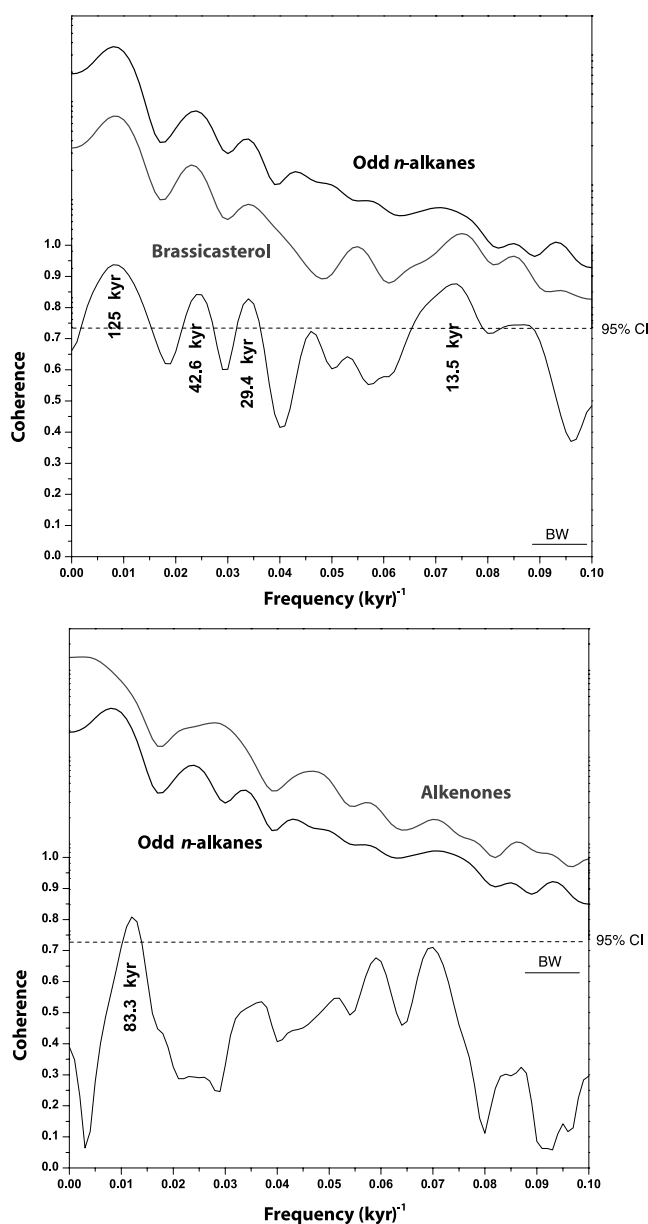


Figure 4. Results of spectral analyses of total odd *n*-alkanes, C₃₇ alkenones, and brassicasterol records. (top) Cross-spectral analysis of long chain *n*-alkanes and brassicasterol shows strong coherence to the eccentricity (100 kyr cycle) and obliquity (41 kyr) bands. (bottom) Cross-spectral analysis of odd carbon number *n*-alkanes and alkenones shows no response to any of the orbital parameters. Dashed line represents the nonzero coherence at the 95% level. BW indicates bandwidth.

[17] The analysis of two additional biomarkers also corroborates the independent behavior of coccolithophorid productivity when compared to other planktonic species. Dinosterol and cholesterol abundances display a parallel trend to that shown by the brassicasterol record with the highest values recorded during glacial periods (Figure 6). The low-dinosterol concentrations registered through the whole

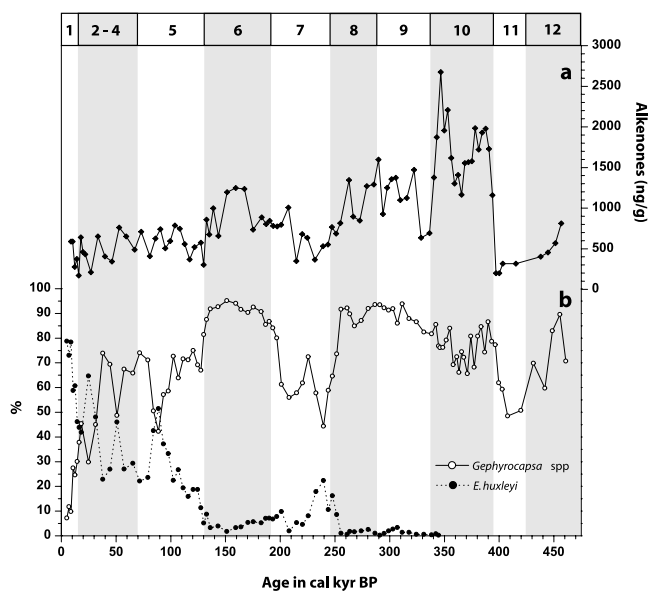


Figure 5. Comparison of (a) C_{37} alkenones concentrations with (b) relative abundances (%) of *Emiliana huxleyi* and *Gephyrocapsa* spp. *Gephyrocapsa* spp. include all species of this genus found in core Fr94-GC3 (*G. muelleriae*, *G. oceanica*, *G. aperta*, *G. caribbeanica*, *G. ericonii*, and *G. sp.* (closed) [Hiramatsu and De Deckker, 1997]). Prior to the first appearance of *E. huxleyi*, species of the genus *Gephyrocapsa* are the most likely contributors of alkenones to the sedimentary record.

record (which sometimes made difficult its quantification) may indicate a minor contribution of dinoflagellates to total productivity. Despite the low concentration of some sections, the observed variability generally matches the glacial/interglacial changes recognized in the brassicasterol record. On the other hand, the occurrence of cholesterol is more difficult to interpret due to the wide variety of precursor organisms. Cholesterol is one of the most abundant sterols in the marine environment and has been generally related to zooplankton productivity, although it has also been found in many diatoms, dinoflagellates and haptophytes [Volkman, 1986]. In core Fr94-GC3, cholesterol concentrations peaked during glacial periods, at times when both brassicasterol and dinosterol values were also higher (Figure 6). The lack of similarity with the alkenone record suggests that coccolithophores were not a significant source of cholesterol. Otherwise, the high alkenone abundances displayed during glacial MIS 10 should also be translated into high cholesterol concentrations and, on the contrary, it is during this glacial period when cholesterol values are the lowest of all four glacial periods. Thus the common productivity pattern illustrated by brassicasterol, dinosterol and cholesterol records suggest that cholesterol was mainly derived by diatoms and/or dinoflagellates or, alternatively, it can be interpreted as a tracer of zooplankton productivity. In any case, these results further illustrate the generally independent pattern of coccolithophorid productivity when compared with the rest of the assessed organisms, which followed a consistent and uniform trend closely linked to changes in dust inputs.

[18] Interpretation of molecular biomarker data as reflecting productivity or continental input can be hampered by potential effects of differential degradation of these compounds on the sedimentary record. Long chain alkanes and alkenones are among the most refractory compounds because of their chain length and the unusual transconfiguration of the double bounds in the alkenones and thus tend to be selectively better preserved in the sediment [Wakeham *et al.*, 1997]. Owing to the similar stability of these two series of compounds, it is expected that any diagenetic effect should be recorded equally on both the *n*-alkane and alkenone records. In core Fr94-GC3, the increase in alkenone concentrations in the older sections suggests that degradation is not overriding the original

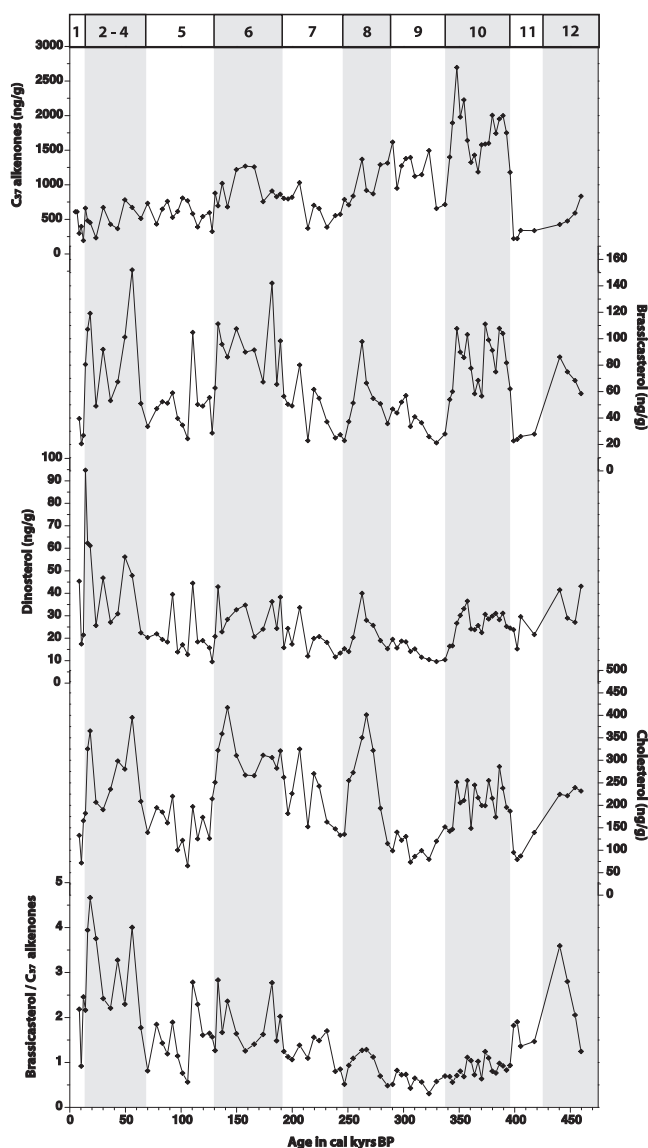


Figure 6. Concentrations of the marine biomarkers analyzed in this study (C_{37} alkenones, brassicasterol, dinosterol, and cholesterol) together with the brassicasterol/ C_{37} alkenone ratio. This ratio has been calculated after normalizing each biomarker to its highest abundance value.

alkenone signal. More importantly, the different pattern displayed by the alkenone and the *n*-alkane records further corroborates the absence of a major postdepositional effect, which would have equally affected both records. Concerning sterols, the existence of functional groups makes them more reactive than *n*-alkanes or alkenones. However, a selective degradation of sterols would not explain the good correlation between *n*-alkanes (which seems not to be significantly affected by diagenesis, as discussed above) and, for instance, brassicasterol (Figure 3), suggesting that differential degradation is not dominating our biomarker records.

4.3. The “Silica Hypothesis”

[19] The “silica hypothesis” suggests that, during glacial times, diatom productivity would be favored over coccolithophores due to an increased availability of Fe and Si from aeolian inputs. The resulting decrease in calcite production would draw down atmospheric CO₂ levels to glacial values through an increase in ocean alkalinity and pH [Archer *et al.*, 2000; Harrison, 2000; Nozaki and Yamamoto, 2001; Tréguer and Pondaven, 2000]. Our results corroborate the expected shift in the relative abundance of siliceous over calcareous organisms induced by higher glacial dust inputs during the last three glacial periods. However, a complete displacement of coccolithophores by diatoms did not occur (Figure 3). During glacial times, brassicasterol concentrations were consistently higher (about 3 times those recorded during interglacials) and tightly coupled to enhanced dust inputs. The enhanced diatom productivity contrasts with the decreasing trend of alkenone abundances through the record, with no evident glacial/interglacial imprint (Figures 3 and 4). Similar differences between these two biomarkers were also encountered for the last two deglaciations in a subantarctic core taken south of our core location [Ikehara *et al.*, 2000].

[20] Archer and Maier-Reimer [1994] suggested that the 80 ppm difference between glacial and interglacial CO₂ levels could be explained by a 40% decrease in calcite production. For this premise to be fully accomplished, our observed higher diatom productivity during glacial periods should have been accompanied by a significant decrease in calcite deposition, which is not evident in our alkenone record. Nonetheless, even if diatoms did not totally displace coccolithophores, the observed glacial change in phytoplankton composition with an increase in diatoms population would have still contributed to the lowering of CaCO₃/organic carbon rain ratio. The increase in organic matter reaching the seafloor would increase alkalinity through degradation of the organic carbon and CaCO₃ dissolution which, in turn, would contribute to some extent in lowering CO₂ concentrations. The lack of a glacial/interglacial pattern in the alkenone record indicates that this mechanism was not equally effective for all glacial periods. For example, the high alkenone abundances recorded during MIS 10 suggest that alkenone-containing coccolithophores were particularly predominant in this region during this time, even when compared with the previous and following interglacials (MIS 11 and 9; Figure 3). Since glacial CO₂ levels during MIS 10 were similar to those observed during

more recent glacial periods [Petit *et al.*, 1999], other mechanisms must have played a more important role in driving atmospheric CO₂ changes.

[21] Recently, Brzezinski *et al.* [2002] suggested an alternative mechanism to enhance diatom productivity through a more efficient redistribution of available dissolved Si. Today, most of the upwelled silicic acid is consumed by diatoms in the Antarctic waters, south of the polar front and only a small amount is transported northward into the subantarctic, limiting diatom production in these waters. During glacial times, with the release of iron and the reduced Si:N uptake ratios of diatoms [Franck *et al.*, 2000], Antarctic diatoms would have exported organic carbon more efficiently, leaving behind unused silicic acid available to be transported to subantarctic waters and farther north [Brzezinski *et al.*, 2002]. This increased supply of dissolved Si would have enhanced diatom productivity in waters as far as the subtropics, with the consequent displacement of coccolithophores. Silicon isotope measurements of diatoms ($\delta^{30}\text{Si}$) from Antarctic sediments show a decrease in Si utilization during glacial times [Brzezinski *et al.*, 2002; De La Rocha *et al.*, 1998], which would also support this “silicic acid leakage” scenario [Matsumoto *et al.*, 2002]. A crucial role of the Southern Ocean in the distribution of nutrients has recently been emphasized by Sarmiento *et al.* [2004], which identifies this region as the main return path of nutrients from the deep ocean to most of the ocean’s surface waters. In the context of our results, this scenario, together with the increased Fe and Si eolian inputs, could certainly explain as well the increase in diatom abundances observed in the location of core Fr94-GC3 during glacial times.

5. Conclusions

[22] Concentrations of long chain *n*-alkanes, C₃₇ alkenones, brassicasterol, dinosterol and cholesterol have been used to assess past glacial/interglacial changes in phytoplankton composition due to changes in continental dust inputs. Our results reveal that diatom productivity responded to changes in dust input, with an increased relative abundance of diatoms versus coccolithophores during the last three glacial periods. However, our alkenone record does not show any significant glacial decrease in coccolithophorid productivity. Thus in the studied area, diatoms apparently did not totally displace coccolithophores as required by the silica hypothesis in order to account for the full glacial/interglacial atmospheric CO₂ change [Harrison, 2000]. Nonetheless, and despite the fact that the carbonate pump was still effective during glacial times, at least in this area of the Southern Hemisphere, the enhanced diatom productivity represented a shift in the CaCO₃/Corg ratio which would still have partly contributed to reduce atmospheric CO₂ concentrations [Archer *et al.*, 2000; Bopp *et al.*, 2003; Matsumoto *et al.*, 2002].

[23] This study illustrates the potential of using molecular biomarkers to elucidate changes in the composition of the phytoplankton community to help understand the role of marine biota in sequestration of atmospheric CO₂. The application of this approach in other oceanic areas could

help to obtain a global picture for the contribution of phytoplankton in regulating past atmospheric CO₂ changes. Lower latitudes of the subtropical and tropical Pacific would be of particular interest to test the silica hypothesis and the “silicic acid leakage” scenario, which suggests an increased Si availability in these areas during glacial times [Brzezinski et al., 2002; Matsumoto et al., 2002].

[24] **Acknowledgments.** We thank A. Moreno and L. Sbaiffi for constructive comments on this manuscript. We are grateful to C. Hiramatsu for useful discussions regarding nannoplankton data and L. Peterson, J. Volkman, and A. Benthien for thorough reviews that significantly improved the manuscript. E.C. and C.P. acknowledge funding from Secretaria de Estado de Educación y Universidades and ARC. G.A.L. published with permission of the CEO of Geoscience Australia. An ARC grant to P.D.D. helped finance the stable isotope analyses. We are also grateful to the Australian National Facilities for use of the R/V *Franklin* to obtain core Fr94GC3.

References

- Anderson, R. F., Z. Chase, M. Q. Fleisher, and J. Sachs (2002), The Southern Ocean's biological pump during the Last Glacial Maximum, *Deep Sea Research Part II*, *49*, 1909–1938.
- Archer, D., and E. Maier-Reimer (1994), Effect of deep-sea sedimentary calcite preservation on atmospheric CO₂ concentration, *Nature*, *367*, 260–263.
- Archer, D., A. Winguth, D. W. Lea, and N. Mahowald (2000), What caused the glacial/interglacial atmospheric pCO₂ cycles?, *Rev. Geophys.*, *38*, 159–189.
- Belkin, I. M., and A. L. Gordon (1996), Southern Ocean fronts from the Greenwich meridian to Tasmania, *J. Geophys. Res.*, *101*, 3675–3696.
- Boon, J. J., W. I. C. Rijpstra, F. Lange, J. W. de Leeuw, M. Yoshioka, and Y. Shimizu (1979), Black Sea sterol—A molecular fossil for dinoflagellate blooms, *Nature*, *277*, 125–127.
- Bopp, L., K. E. Kohfeld, C. Le Quéré, and O. Aumont (2003), Dust impact on marine biota and atmospheric CO₂ during glacial periods, *Paleoceanography*, *18*(2), 1046, doi:10.1029/2002PA000810.
- Boyd, P. W., et al. (2000), A mesoscale phytoplankton bloom in the polar Southern Ocean stimulated by iron fertilization, *Nature*, *407*, 695–702.
- Brassell, S. C. (1993), Applications of biomarkers for delineating marine paleoclimatic fluctuations during the Pleistocene, in *Organic Geochemistry: Principles and Applications*, edited by M. H. Engel and S. A. Macko, pp. 699–738, Plenum, New York.
- Brzezinski, M. A., C. J. Pride, V. M. Franck, D. M. Sigman, J. Sarmiento, K. Matsumoto, N. Gruber, G. H. Rau, and K. H. Coale (2002), A switch from Si(OH)₄ to NO₃⁻ depletion in the glacial Southern Ocean, *Geophys. Res. Lett.*, *29*, 1564, doi:10.1029/2001GL014349.
- Calvo, E., C. Pelejero, and G. A. Logan (2003), Pressurized liquid extraction of selected molecular biomarkers in deep sea sediments used as proxies in paleoceanography, *J. Chromatogr. A*, *989*, 197–205.
- Coale, K. H., et al. (1996), A massive phytoplankton bloom induced by ecosystem-scale iron fertilization experiment in the equatorial Pacific Ocean, *Nature*, *383*, 495–501.
- Conte, M. H., A. Thompson, D. Lesley, and R. P. Harris (1998), Genetic and physiological influences on the alkenone/alkenoate versus growth temperature relationship in *Emiliania huxleyi* and *Gephyrocapsa oceanica*, *Geochim. Cosmochim. Acta*, *62*, 51–68.
- Cranwell, P. A. (1973), Chain-length distribution of *n*-alkanes from lake sediments in relation to post-glacial environmental change, *Freshwater Biol.*, *3*, 259–265.
- Cranwell, P. A., G. Eglinton, and N. Robinson (1987), Lipids of aquatic organisms as potential contributors to lacustrine sediments-II, *Org. Geochem.*, *11*, 513–527.
- De La Rocha, C. L., M. A. Brzezinski, M. J. DeNiro, and A. Shemesh (1998), Silicon-isotope composition of diatoms as an indicator of past oceanic change, *Nature*, *395*, 680–683.
- Dodd, R. S., and Z. A. Afzal-Rafii (2000), Habitat-related adaptive properties of plant cuticular lipids, *Evolution*, *54*, 1438–1444.
- Dodd, R. S., Z. A. Rafii, and A. B. Power (1998), Ecotypic adaptation in *Austrocedrus chilensis* in cuticular hydrocarbon composition, *New Phytol.*, *138*, 699–708.
- EGGE, J. K., and D. L. Aksnes (1992), Silicate as a regulating nutrient in phytoplankton competition, *Mar. Ecol. Prog. Ser.*, *83*, 281–289.
- Eglinton, G., and R. J. Hamilton (1967), Leaf epicuticular waxes, *Science*, *156*, 1322–1335.
- Fischer, E., F. Oldfield, R. Wake, J. Boyle, P. Appleby, and G. A. Wolff (2003), Molecular marker records of land use change, *Org. Geochem.*, *34*, 105–119.
- Franck, V. M., M. A. Brzezinski, K. H. Coale, and D. M. Nelson (2000), Iron and silicic acid concentrations regulate Si uptake north and south of the polar frontal zone in the Pacific sector of the Southern Ocean, *Deep Sea Research Part II*, *47*, 3315–3338.
- Gagosian, R. B., E. T. Peltzer, and J. T. Merrill (1987), Long-range transport of terrestrially derived lipids in aerosols from the South Pacific, *Nature*, *325*, 800–803.
- Harle, K. J. (1997), Late Quaternary vegetation and climate change in southeastern Australia: Palynological evidence from marine core E55-6, *Palaeogeogr. Palaeoclimatol. Palaeoecol.*, *131*, 465–483.
- Harrison, K. G. (2000), Role of increased marine silica input on paleo-pCO₂ levels, *Paleoceanography*, *15*, 292–298.
- Hesse, P. P. (1994), The record of continental dust from Australia in Tasman Sea sediments, *Quat. Sci. Rev.*, *13*, 257–272.
- Hesse, P. P., and G. H. McTainsh (1999), Last Glacial Maximum to early Holocene wind strength in the mid-latitudes of the Southern Hemisphere from aeolian dust in the Tasman Sea, *Quat. Res.*, *52*, 343–349.
- Hiramatsu, C., and P. De Deckker (1997), The late Quaternary calcareous nannoplankton assemblages from three cores from the Tasman Sea, *Palaeogeogr. Palaeoclimatol. Palaeoecol.*, *131*, 391–412.
- Hutchins, D. A., and K. W. Bruland (1998), Iron-limited diatom growth and Si:N uptake ratios in a coastal upwelling regime, *Nature*, *393*, 561–564.
- Ikehara, M., K. Kawamura, N. Ohkouchi, M. Murayama, T. Nakamura, and A. Taira (2000), Variations of terrestrial input and marine productivity in the Southern Ocean (48°S) during the last two deglaciations, *Paleoceanography*, *15*, 170–180.
- Imbrie, J., J. D. Hays, D. G. Martinson, A. McIntyre, A. C. Mix, J. J. Morley, N. G. Pisias, W. L. Prell, and N. J. Shackleton (1984), The orbital theory of Pleistocene climate: Support from a revised chronology of the marine δ¹⁸O record, in *Milankovitch and Climate, Part 1*, edited by A. L. Berger et al., pp. 269–305, D. Reidel, Norwell, Mass.
- Knox, F., and M. B. McElroy (1984), Changes in atmospheric CO₂ influence of the marine biota at high latitude, *J. Geophys. Res.*, *89*, 4629–4637.
- Kumar, N., R. F. Anderson, R. A. Mortlock, P. N. Froelich, P. Kubik, H. B. Ditttrich, and M. Suter (1995), Increased biological productivity and export production in the glacial Southern Ocean, *Nature*, *378*, 675–680.
- Mahowald, N., K. E. Kohfeld, M. Hansson, Y. Balkanski, C. G. A. Harrison, I. C. Prentice, M. Schulz, and H. Rodhe (1999), Dust sources and deposition during the last glacial maximum and current climate: A comparison of model results with paleodata from ice cores and marine sediments, *J. Geophys. Res.*, *104*, 15,895–15,916.
- Marlowe, I. T., S. C. Brassell, G. Eglinton, and J. C. Green (1990), Long-chain alkenones and alkyl alkenoates and the fossil coccolith record of marine sediments, *Chem. Geol.*, *88*, 349–375.
- Martin, J. H. (1990), Glacial-interglacial CO₂ change: The iron hypothesis, *Paleoceanography*, *5*, 1–13.
- Martin, J. H., and S. E. Fitzwater (1988), Iron deficiency limits phytoplankton growth in the north-east Pacific subarctic, *Nature*, *331*, 341–343.
- Martin, J. H., R. M. Gordon, and S. E. Fitzwater (1990), Iron in Antarctic waters, *Nature*, *345*, 156–158.
- Martin, J. H., et al. (1994), Testing the iron hypothesis in ecosystems of the equatorial Pacific Ocean, *Nature*, *371*, 123–129.
- Martinez, J. I. (1994), Late Pleistocene paleoceanography of the Tasman Sea: Implications for the dynamics of the warm pool in the western Pacific, *Palaeogeogr. Palaeoclimatol. Palaeoecol.*, *112*, 19–62.
- Martinson, D. G., N. G. Pisias, J. D. Hays, J. J. Imbrie, T. C. Moore, and N. J. Shackleton (1987), Age dating and the orbital theory of the ice ages: Development of a high-resolution 0 to 300,000 year chronostratigraphy, *Quat. Res.*, *27*, 1–29.
- Matsumoto, K., J. Sarmiento, and M. Brzezinski (2002), Silicic acid leakage from the Southern Ocean: A possible explanation for glacial atmospheric pCO₂, *Global Biogeochem. Cycles*, *16*(3), 1031, doi:10.1029/2001GB001442.
- Müller, P. J., M. Cepek, G. Ruhland, and R. Schneider (1997), Alkenone and coccolithophorid species changes in Late Quaternary sediments from the Walvis Ridge: Implications

- for the alkenone paleotemperature method, *Palaogeogr. Palaeoclimatol. Palaeoecol.*, **135**, 71–96.
- Müller, P. J., G. Kirst, G. Ruhland, I. von Storch, and A. Rosell-Melé (1998), Calibration of the alkenone paleotemperature index U_{37}^K based on core-tops from the eastern South Atlantic and the global ocean (60°N–60°S), *Geochim. Cosmochim. Acta*, **62**, 1757–1772.
- Nees, S. (1997), Late Quaternary palaeoceanography of the Tasman Sea: The benthic foraminiferal view, *Palaogeogr. Palaeoclimatol. Palaeoecol.*, **131**, 365–389.
- Nees, S., L. Armand, P. De Deckker, M. Labracherie, and V. Passlow (1999), A diatom and benthic foraminiferal record from the south Tasman Rise (southeastern Indian Ocean); implications for palaeoceanographic changes for the last 200,000 years, *Mar. Micropaleontol.*, **38**, 69–89.
- Nozaki, Y., and Y. Yamamoto (2001), Radium 228 based nitrate fluxes in the eastern Indian Ocean and the South China Sea and a silicon-induced “alkalinity pump” hypothesis, *Global Biogeochem. Cycles*, **15**, 555–567.
- Pailller, D., E. Bard, F. Rostek, Y. Zheng, R. Mortlock, and A. Van Geen (2002), Burial of redox-sensitive metals and organic matter in the equatorial Indian Ocean linked to precession, *Geochim. Cosmochim. Acta*, **66**, 849–865.
- Passlow, V., P. Wang, and A. R. Chivas (1997), Late Quaternary palaeoceanography near Tasmania, southern Australia, *Palaogeogr. Palaeoclimatol. Palaeoecol.*, **131**, 433–463.
- Pelejero, C. (2003), Terrigenous *n*-alkane input in the South China Sea: High-resolution records and surface sediments, *Chem. Geol.*, **200**, 89–103.
- Peltzer, E. T., and R. B. Gagosian (1989), Organic geochemistry of aerosols over the Pacific Ocean, in *Chemical Oceanography*, edited by J. P. Riley and R. Chester, pp. 281–328, Academic, San Diego, Calif.
- Petit, J. R., et al. (1999), Climate and atmospheric history of the past 420,000 years from the Vostok ice core, Antarctica, *Nature*, **399**, 429–436.
- Poynter, J. G., P. Farrimond, N. Robinson, and G. Eglinton (1989), Aeolian-derived higher plant lipids in the marine sedimentary record: Links with palaeoclimate, in *Paleoclimatology and Paleometeorology: Modern and Past Patterns of Global Atmospheric Transport*, edited by M. Leinen and M. Samthein, pp. 435–462, Kluwer Acad., Norwell, Mass.
- Rea, D. K. (1994), The paleoclimatic record provided by eolian deposition in the deep sea: The geologic history of wind, *Rev. Geophys.*, **32**, 159–195.
- Rintoul, S. R., J. R. Donguy, and D. H. Roemmich (1997), Seasonal evolution of upper ocean thermal structure between Tasmania and Antarctica, *Deep Sea Res. Part I*, **44**, 1185–1202.
- Sarmiento, J., and J. R. Toggweiler (1984), A new model for the role of the oceans in determining atmospheric carbon dioxide, *Nature*, **308**, 621–624.
- Sarmiento, J. L., N. Gruber, M. A. Brzezinski, and J. P. Dunne (2004), High-latitude controls of thermocline nutrients and low latitude biological productivity, *Nature*, **427**, 56–60.
- Sawada, K., N. Handa, Y. Shiraiwa, A. Danbara, and S. Montani (1996), Long-chain alkenones and alkyl alkenoates in the coastal and pelagic sediments of the northwest North Pacific, with special reference to the reconstruction of *Emiliania huxleyi* and *Gephyrocapsa oceanica* ratios, *Org. Geochem.*, **24**, 751–764.
- Schubert, C. J., J. Villanueva, S. E. Calvert, G. L. Cowie, U. von Rad, H. Schulz, and U. Berner (1998), Stable phytoplankton community in the Arabian Sea over the last 200,000 years, *Nature*, **394**, 563–566.
- Schulte, S., F. Rostek, E. Bard, J. Rullkötter, and O. Marchal (1999), Variations of oxygen-minimum and primary productivity recorded in sediments of the Arabian Sea, *Earth Planet. Sci. Lett.*, **173**, 205–221.
- Sedwick, P. N., P. R. Edwards, D. J. Mackey, F. B. Griffiths, and J. S. Parslow (1997), Iron and manganese in surface waters of the Australian subantarctic region, *Deep Sea Res. Part I*, **44**, 1239–1253.
- Takeda, S. (1998), Influence of iron availability on nutrient consumption ratio of diatoms in oceanic waters, *Nature*, **393**, 774–777.
- Thierstein, H. R., K. R. Geitzenauer, B. Molino, and N. J. Shackleton (1977), Global synchronicity of late Quaternary coccolith datum levels: Validation by oxygen isotopes, *Geology*, **5**, 400–404.
- Tréguer, P., and P. Pondaven (2000), Silica control of carbon dioxide, *Nature*, **406**, 358–359.
- Tréguer, P., D. M. Nelson, A. J. Vanbennekorn, D. J. Demaster, A. Leynaert, and B. Queguiner (1995), The silica balance in the world ocean: A reestimate, *Science*, **268**, 375–379.
- Tsuda, A. S., et al. (2003), A mesoscale iron enrichment in the western subarctic Pacific induces a large centric diatom bloom, *Science*, **300**, 958–961.
- Villanueva, J., E. Calvo, C. Pelejero, J. O. Grimalt, A. Boelaert, and L. Labeyrie (2001), A latitudinal productivity band in the central North Atlantic over the last 270 kyr: An alkenone perspective, *Paleoceanography*, **16**, 617–626.
- Volkman, J. K. (1986), A review of sterol markers for marine and terrigenous organic matter, *Org. Geochem.*, **9**, 83–99.
- Volkman, J. K., S. M. Barrett, S. I. Blackburn, and E. L. Sikes (1995), Alkenones in *Gephyrocapsa oceanica*: Implications for studies of paleoclimate, *Geochim. Cosmochim. Acta*, **59**, 513–520.
- Wakeham, S. G., C. Lee, J. I. Hedges, P. J. Hernes, and M. L. Peterson (1997), Molecular indicators of diagenetic status in marine organic matter, *Geochim. Cosmochim. Acta*, **61**, 5363–5369.
- Watson, A. J., D. C. E. Bakker, A. J. Ridgwell, P. W. Boyd, and C. S. Law (2000), Effect of iron supply on Southern Ocean CO₂ uptake and implications for glacial atmospheric CO₂, *Nature*, **407**, 730–733.
- Werne, J. P., D. J. Hollander, T. W. Lyons, and L. C. Peterson (2000), Climate-induced variations in productivity and planktonic ecosystem structure from the Younger Dryas to Holocene in the Cariaco Basin, Venezuela, *Paleoceanography*, **15**, 19–29.
- Wyrski, K. (1962), The subsurface water masses in the western South Pacific Ocean, *Aust. J. Mar. Freshwater Res.*, **13**, 18–47.
- Wyrwoll, K. H., B. Dong, and P. Valdes (2000), On the position of Southern Hemisphere westerlies at the last glacial maximum; an outline of AGCM simulation results and evaluation of their implications, *Quat. Sci. Rev.*, **19**, 881–898.

E. Calvo and C. Pelejero, Research School of Earth Sciences, Australian National University, Canberra, ACT 0200, Australia. (eva.calvo@anu.edu.au)

P. De Deckker, Department of Geology, Australian National University, Canberra ACT 0200, Australia.

G. A. Logan, Petroleum and Marine Division, Geosciences Australia, GPO Box 378, Canberra, ACT 2601, Australia.